Non-resonant Higgs Pair Production and Higgs self couplings limits by ATLAS

Luis Falda Coelho[a,*], **on behalf of the ATLAS Collaboration**

[a] *Brandeis University, Waltham, MA, United States*

E-mail: lfaldaul@cern.ch

In the Standard Model (SM), the ground state of the Higgs field is not found at zero but instead corresponds to one of the degenerate solutions minimising the Higgs potential. In turn, this spontaneous electroweak symmetry breaking provides a mechanism for the mass generation of nearly all fundamental particles. The SM makes a definite prediction for the Higgs boson self-coupling and thereby the shape of the Higgs potential. Experimentally, both can be probed through the production of Higgs boson pairs (HH), a rare process that presently receives a lot of attention at the LHC. In this note, the latest HH searches by the ATLAS experiment are reported. Non-resonant HH search results are interpreted both in terms of sensitivity to the SM and as limits on the Higgs boson self-coupling and the quartic $VVHH$ coupling. Additionally, extrapolations of recent HH results towards the High-Luminosity LHC upgrade are also discussed.

Presented at the 32nd International Symposium on Lepton Photon Interactions at High Energies,
Madison, Wisconsin, USA,
August 25-29, 2025

1. Introduction

Since the Higgs boson's observation [1, 2] by the ATLAS [3] and CMS [4] collaborations, a primary objective of the LHC program has been the precise measurement of its properties and their consistency with the Standard Model (SM). While all measurements to date agree with SM predictions within uncertainties, unresolved fundamental questions imply physics beyond the SM likely exists. The Higgs sector is a particularly promising area for such discoveries, offering a direct window into electroweak symmetry breaking [5–10].

Experimental measurements so far probe Higgs interactions near the minimum of its potential, but its full structure remains untested. Access to the Higgs self-coupling, measurable through Higgs boson pair production (HH), provides a direct probe of this potential. However, HH production is rare, with cross-sections about three orders of magnitude smaller than single-Higgs production. HH production occurs through gluon fusion (ggF), vector-boson fusion (VBF), and associated production with top quarks ($t\bar{t}HH$) or vector bosons (VHH).

Searches target a few key decay channels that balance branching fraction and experimentally clean signatures. The $HH \to b\bar{b}b\bar{b}$ mode has the largest rate ($\sim$ 34%) but suffers from severe multijet backgrounds, while $HH \to b\bar{b}\gamma\gamma$ offers an exceptionally clean signature despite its small branching fraction ($\sim$ 0.3%). The $HH \to b\bar{b}\tau^+\tau^-$ channel, with a moderate branching fraction ($\sim$ 7%) and lower background, currently provides the most stringent individual limits on HH production [16].

New physics could alter Higgs couplings, enhancing HH production by over an order of magnitude. Measuring this process is therefore a powerful probe of the scalar sector and a central objective of Run 3 and the HL-LHC program.

2. Full Run 2 HH Combination

Six analyses searching for HH production in the $b\bar{b}\tau\tau$, $b\bar{b}\gamma\gamma$, $b\bar{b}b\bar{b}$, multilepton, and $b\bar{b}ll$+E_T^{miss} final states, using the full Run-2 dataset of up to 140 fb^{-1} at a center-of-mass energy of $\sqrt{s}$ = 13 TeV, were statistically combined [16]. The combination was performed for non-resonant ggF and VBF production, yielding an observed (expected) upper limit on the HH production rate of 2.9 (2.4) times the SM prediction at 95% confidence-level (CL). The upper limits show a 17% improvement compared to the previously published combination [17], with approximately 4% gain resulting from the inclusion of newly added channels, namely the multilepton and $b\bar{b}\ell\ell + E_T^{\text{miss}}$ final states.

Constraints were also set on the ratio $k_\lambda = \lambda_{HHH}/\lambda_{HHH}^{SM}$ of the Higgs boson self-coupling to its SM value, as well as on the quartic coupling modifier $k_{2V} = \lambda_{HHVV}/\lambda_{HHVV}^{SM}$. The observed (expected) 95% CL intervals are $-1.2 < k_\lambda < 7.2$ ($-1.6 < k_\lambda < 7.2$) for the self-coupling, and $0.6 < k_{2V} < 1.5$ ($0.4 < k_{2V} < 1.6$) for the $HHVV$ coupling. The leading contribution to the limits on k_{2V} coupling modifier comes from the $b\bar{b}b\bar{b}$ boosted VBF channel, while $b\bar{b}\gamma\gamma$ provides the leading contribution to the limits on k_λ.

3. Full Run 2 + Partial Run 3 $HH \to b\bar{b}\gamma\gamma$ Analysis

A recent update of the $b\bar{b}\gamma\gamma$ search incorporates partial Run 3 data along with improvements in analysis techniques and object reconstruction [18]. The study uses the full Run 2 dataset together with the partial Run 3 dataset, corresponding to a total integrated luminosity of 308 fb^{-1}. This includes 140 fb^{-1} at $\sqrt{s}$ = 13 TeV, collected between 2015 and 2018, and 168 fb^{-1} at 13.6 TeV, collected between 2022 and 2024.

The best-fit signal strength is determined to be $\mu_{HH} = 0.9^{+1.3}_{-1.0}\,(\text{stat.})^{+0.6}_{-0.5}\,(\text{syst.})$, with an expected value of $\mu_{HH} = 1.0^{+1.3}_{-1.0}$ times the SM. Separate fits to Run 2 and Run 3 data yield compatible results, with a combined p-value of 0.37. The observed (expected) statistical significance of the signal is 0.84 σ (1.01 σ). Systematic uncertainties are primarily driven by the modelling of heavy-flavour contributions in single Higgs production, photon energy scale and resolution, and the theoretical prediction of the Higgs-pair cross section. A 95% CL upper limit on the signal strength is set at $\mu_{HH} < 3.8$, assuming SM HH production. In the background-only hypothesis, the expected limit is $\mu_{HH} < 2.6$, while when assuming $\mu_{HH} = 1$ the expected limit becomes $\mu_{HH} < 3.7$. The limits are found to be comparable in sensitivity to those from the full Run 2 HH combination.

Figure 1 presents the fit results for Run 2 and Run 3 individually, as well as their statistical combination, showing both the discovery significance and the 95% CL upper limit.

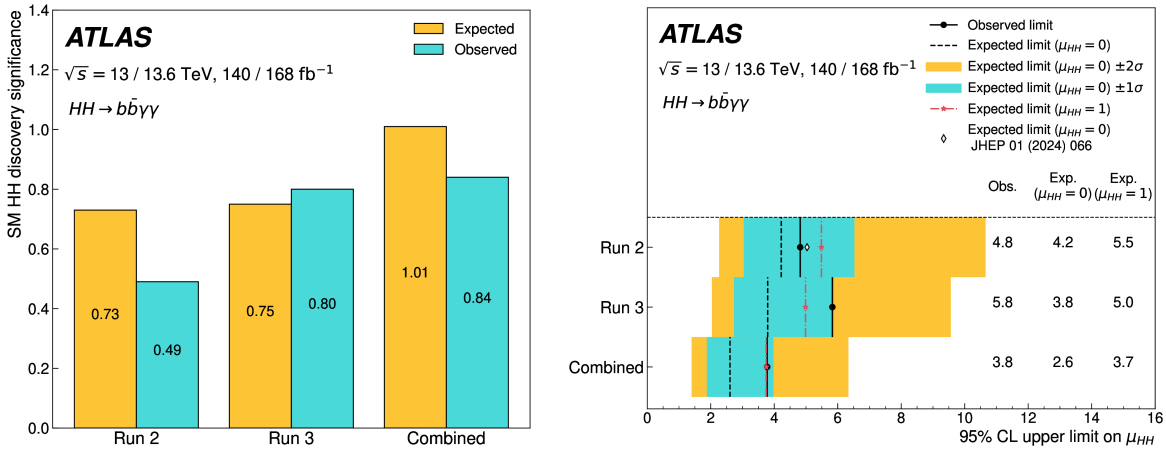

(a) **(b)**

Figure 1: (a) Observed and expected statistical significance of the HH signal, and (b) the 95% CL upper limits on the signal strength, obtained with fits to Run 2 and Run 3 data as well as their combination [18].

Compared to the previous result [19], the observed significance improves by approximately 20%. This enhancement is largely due to a new transformer-based b-tagging algorithm (GN2), which provides improved light-jet and c-jet rejection. This also allows for the use of a looser b-jet selection operating at an 85% working point, increasing the signal acceptance. An additional 5% gain originates from a kinematic fit that improves the resolution of the $b\bar{b}$ and $b\bar{b}b\bar{b}$ invariant masses. The inclusion of the new dataset from Run 3 contributes to roughly 60% of the total improvement. This is decomposed into a 50% contribution from the increased integrated luminosity and a further 10% from an optimised categorisation strategy that benefits from correlating the background shapes across the two data-taking periods.

The analysis is further interpreted within the Higgs Effective Field Theory (HEFT) framework, including the impact of EFT operators on VBF HH production. Likelihood scans of individual anomalous couplings, profiling over others, reveal strong correlations among the three main HEFT operators, as shown in Fig. 2a. The results are also expressed in the Standard Model Effective Field Theory (SMEFT) framework, comparing linear-only and linear+quadratic truncation schemes for each Wilson coefficient. This comparison tests the SMEFT expansion's validity and potential dimension-8 effects, illustrated in Fig. 2b for c_H at $\Lambda = 1$ TeV.

4. First Search for Triple-Higgs Production

ATLAS has established the first limits on triple-Higgs boson (HHH) production focusing on the fully-hadronic decay final state consisting of three b-quark pairs ($b\bar{b}b\bar{b}b\bar{b}$) [21]. The analysis is performed using full Run 2 data corresponding to an integrated luminosity of 126 fb^{-1}. Both nonresonant and resonant HHH production mechanisms were investigated. The nonresonant analysis can provide the only direct access to the quartic Higgs boson self-couplings.

Deep Neural Network (DNN) classifiers are trained to separate signal from the dominant multijet background, using kinematic properties of the reconstructed Higgs boson candidates as input. The reconstruction is formed by pairing jets with a χ^2-based algorithm that checks compatibility with the Higgs mass assumption. The background estimation is fully data-driven, relying on the extrapolation of DNN score distributions from lower-purity b-jet multiplicity regions into the 6 b-jet signal region, under the assumption that background kinematics are similar across these regions. The final results are derived from a profile likelihood fit to the binned DNN output distributions. Systematic uncertainties associated with the background extrapolation are evaluated by comparing data between the different b-jet multiplicity regions in the low DNN scores.

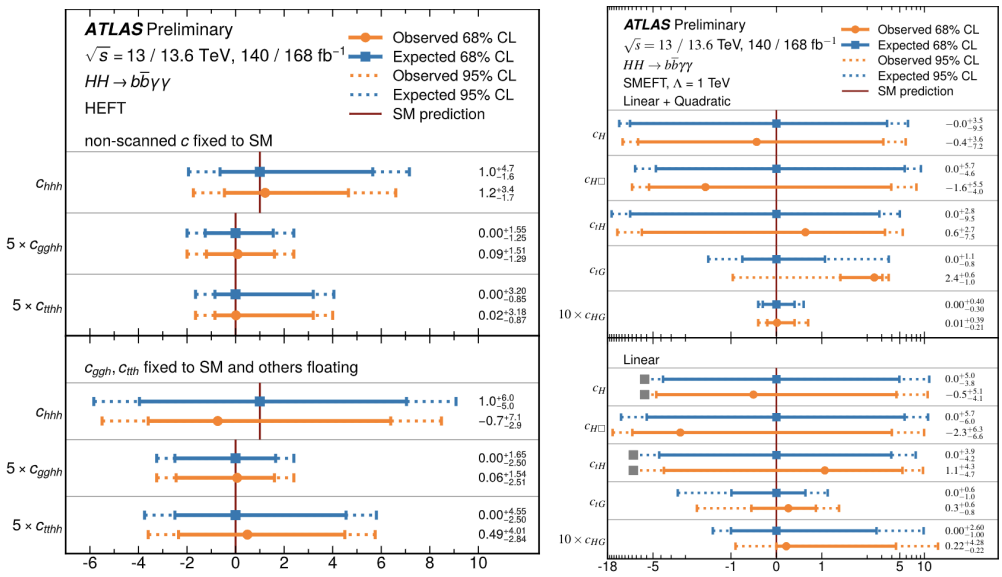

(a) **(b)**

Figure 2: (a) Likelihood scans for the HEFT coefficients. Results are shown for all other coefficients fixed to their SM values, as well as when profiling over the couplings. (b) Likelihood scans for the SMEFT coefficients, using both the linear and linear+quadratic truncation schemes [20].

No significant excess of events over the background prediction is observed. Upper limits on the production cross section are set at 95% CL, including an upper limit of 59 fb on the cross section for SM HHH production. Assuming $\kappa_4 = 1$, the trilinear coupling modifier κ_λ is constrained to be within $-11 < \kappa_\lambda < 17$ at 95% CL. Assuming $\kappa_\lambda = 1$, the quartic coupling modifier κ_4 is restricted to $-230 < \kappa_4 < 240$ at 95% CL.

5. HL-LHC Projections of Full Run 2 Analyses

The HH analyses achieved unprecedented sensitivity to the Higgs boson self-coupling and HH production, well beyond earlier expectations. This was made possible through the enlarged dataset and significant improvements in object reconstruction and analysis strategies. Nevertheless, measuring the Higgs self-coupling remains a central challenge for the HL-LHC physics program.

An ATLAS projection study [22] based on the combination of the $b\bar{b}b\bar{b}$, $b\bar{b}\gamma\gamma$ and $b\bar{b}\tau\tau$ full Run 2 analyses estimated the expected sensitivity at the HL-LHC with 3000 fb^{-1} at $\sqrt{s} = 14$ TeV. Four uncertainty scenarios were considered, ranging from purely statistical to Run 2-like systematic uncertainties. In the scenario referred to as baseline scenario the theory uncertainties are halved and the instrumental uncertainties are reduced to HL-LHC expectation. The production cross-sections of the processes are scaled to the $\sqrt{s} = 14$ TeV expectations. Figure 3a shows the upper limits on the HH production cross-section as a function of the luminosity. Figure 3b shows the projected negative log-profile-likelihood as a function of κ_λ at 3000 fb^{-1}. The study projects a significance for SM HH production of up to 4.3σ in the baseline scenario, with the Higgs self-coupling constrained to $-0.71 < \kappa_\lambda < 1.48$ at 68% CL.

6. Conclusions

Higgs boson pair production serves as a key probe of the electroweak symmetry breaking mechanism, providing direct sensitivity to the Higgs self-coupling. This document has presented the latest results from the ATLAS Collaboration on non-resonant HH production to date. The full Run-2 combination resulted in an observed (expected) 95% CL upper limit of 2.9 (2.4) times the SM cross section. Recent results incorporating partial Run-3 data show improved sensitivity, with the $HH \to b\bar{b}\gamma\gamma$ analysis using 308 fb^{-1} achieving an observed (expected) limit of 3.8 (2.6) times the SM cross section and constraining $-1.7 < \kappa_\lambda < 6.6$ at 95%

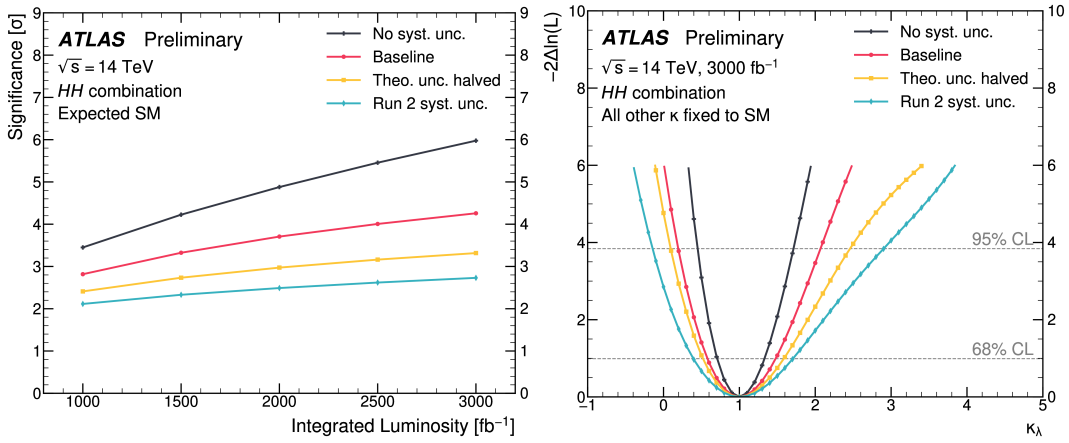

(a) **(b)**

Figure 3: (a) Projected upper limits on the cross-section for SM HH production, combining the $b\bar{b}\gamma\gamma$, $b\bar{b}\tau\tau$ and $b\bar{b}b\bar{b}$ channels for integrated luminosities up to 3000 fb^{-1} at $\sqrt{s}$ = 14 TeV at the HL-LHC. (b) Projected negative log-profile-likelihood as a function of κ_λ. Four uncertainty scenarios are shown [22].

CL. This single channel already delivers sensitivity comparable to the full Run-2 combination. Projections for the High-Luminosity LHC indicate that observation of HH production is within reach for both ATLAS and CMS, and this goal will benefit from continued advancements on object reconstruction, analysis techniques, and increased statistics.

References

[1] ATLAS Collaboration, Phys. Lett. B **716** (2012), doi:10.1016/j.physletb.2012.08.020

[2] CMS Collaboration, Phys. Lett. B **716** (2012), doi:10.1016/j.physletb.2012.08.021

[3] ATLAS Collaboration, 2008 JINST **3** (2008), S08003 doi:10.1088/1748-0221/3/08/S08003

[4] CMS Collaboration, JINST **3** (2008), S08004 doi:10.1088/1748-0221/3/08/S08004

[5] F. Englert and R. Brout, Phys. Rev. Lett. **13**, 321–323 (1964). doi:10.1103/PhysRevLett.13.321

[6] P. W. Higgs, Phys. Lett. **12**, 132–133 (1964). doi:10.1016/0031-9163(64)91136-9

[7] P. W. Higgs, Phys. Rev. Lett. **13**, 508–509 (1964). doi:10.1103/PhysRevLett.13.508

[8] G. S. Guralnik et al., Phys. Rev. Lett. **13**, 585–587 (1964). doi:10.1103/PhysRevLett.13.585

[9] P. W. Higgs, Phys. Rev. **145**, 1156–1163 (1966). doi:10.1103/PhysRev.145.1156

[10] T. W. B. Kibble, Phys. Rev. **155**, 1554–1561 (1967). doi:10.1103/PhysRev.155.1554

[11] M. Grazzini et al., J. High Energy Phys. **2018**, 59 (2018). doi:10.1007/JHEP05(2018)059.

[12] F. A. Dreyer and A. Karlberg, Phys. Rev. D **99**, 074028 (2019). doi:10.1103/PhysRevD.99.074028.

[13] F. A. Dreyer and A. Karlberg, Phys. Rev. D **98**, 114016 (2018). doi:10.1103/PhysRevD.98.114016.

[14] F. A. Dreyer et al., Eur. Phys. J. C **80**, 1037 (2020). doi:10.1140/epjc/s10052-020-08610-7.

[15] R. Frederix et al., Phys. Lett. B **732**, 142–149 (2014). doi:10.1016/j.physletb.2014.03.026.

[16] ATLAS Collaboration, Phys. Rev. Lett. **133** (2024) no.10, 101801 doi:10.1103/PhysRevLett.133.101801

[17] ATLAS Collaboration, Phys. Lett. B **843** (2023), 137745 doi:10.1016/j.physletb.2023.137745

[18] ATLAS Collaboration, arXiv:2507.03495

[19] ATLAS Collaboration, JHEP **01** (2024), 066 doi:10.1007/JHEP01(2024)066

[20] ATLAS Collaboration, ATL-PHYS-PUB-2025-034

[21] ATLAS Collaboration, Phys. Rev. D **111** (2025) no.3, 032006 doi:10.1103/PhysRevD.111.032006

[22] ATLAS Collaboration, ATL-PHYS-PUB-2025-006